A Comparative Correction Method for CFD Numerical Simulation and Wind Tunnel Experiment of Flying Wing Aircraft with Small Aspect Ratio

Liang Xu*, Bin Chen, and Jieke Yao

Chengdu Aircraft Industrial (Group) Co., Ltd, Chengdu, China

*Corresponding author

Abstract

The state and size of the numerical simulation model and the wind tunnel experiment model are different, which makes the aerodynamic data of the aircraft different. In this paper, two sets of longitudinal aerodynamic data are obtained through CFD numerical simulation and wind tunnel experiment for flying wing aircraft with small aspect ratio, the difference between simulation and experiment is analyzed, the comparative correction method of longitudinal aerodynamic coefficient of flying wing aircraft is established, the correction values of lift coefficient and pitching moment coefficient is obtained, and the difference between numerical simulation and wind tunnel experiment data is corrected. The results show that the corrected aerodynamic data of numerical simulation are in good agreement with the wind tunnel experiment, and meet the accuracy requirements of engineering application.

Keywords

CFD, Numerical Simulation, Wind Tunnel Test.

1. Introduction

The flying wing is a kind of aircraft aerodynamic layout different from the conventional aerodynamic layout, the fuselage and the wing are integrated, the tail is eliminated, so that the whole shape is a lift surface. The shape of the flying wing layout aircraft can be designed according to aerodynamic optimal conditions, with high aerodynamic efficiency, large lift-to-drag ratio, and innate low RCS characteristics. Due to its superior aerodynamic, loading, stealth and other capabilities, the flying wing layout has become an ideal layout for bombers and unmanned combat aircraft, etc [1-2].

At present, the aerodynamic data of aircraft are mainly obtained by numerical simulation and wind tunnel experiment. Yue Kuizhi [3] numerically simulated the aerodynamic flow field characteristics of the dual-wing UAV based on the CFD theory. Li Yonghong [4] studied the correlation between the force-measuring experiment data of the small aspect ratio flying wing layout in different wind tunnels and the relationship between the experiment accuracy and the flow characteristics of the flying wing layout. Su Jichuan [5] found the phenomenon of sudden drop of transonic lift and sudden rise of pitching moment in the wind tunnel experiment of small aspect ratio flying wing standard model, analyzed the mechanism of this phenomenon through numerical simulation, and studied the generation, development and rupture process of leading edge vortex of flying wing standard model. Ma Zhenyu [6] studied the three-dimensional viscous flow field characteristics of the wing through numerical simulation and wind tunnel experiment. Liu Yi [7] verified the effect of installing winglets on low-speed aircraft through numerical calculation and wind tunnel experiment, effectively improved the flow field characteristics of wingtips, and increased the cruise lift-drag ratio. Liu Xiaobo [8] studied the factors affecting the aerodynamic characteristics of folding wings by wind tunnel experiment

and numerical methods. Most of the literature studies use the numerical simulation method as a tool to verify the reliability of the wind tunnel experiment results and analyze the reasons for the abnormal experiment phenomena, while the comparative study of the differences between the numerical simulation results and the wind tunnel experiment data is relatively scarce.

In this paper, the CFD numerical simulation and wind tunnel experiments were carried out for flying wing aircraft with small aspect ratio, and two sets of longitudinal aerodynamic data were obtained. By comparing and analyzing the differences between the simulation results and the experiment data, the correction method of the longitudinal aerodynamic coefficient of the flying wing configuration was established, and the correction values of the lift coefficient and the pitching moment coefficient were obtained, the comparative correction of the numerical simulation and wind tunnel experiment data of the flying wing layout are carried out.

2. Comparison of Longitudinal Aerodynamic Characteristics

2.1. Aerodynamic Data Acquisition

Numerical simulation data of small aspect ratio flying wing configuration are obtained by using CFD solver based on N-S equation (as shown in Figure 1), and wind tunnel experiment data are obtained by high and low speed force-measuring wind tunnel experiment (as shown in Figure 2). By comparing and analyzing the two sets of aerodynamic characteristic data, the difference law and relevance correction method between the numerical simulation data and the wind tunnel experiment data of the small aspect ratio flying wing configuration are obtained.

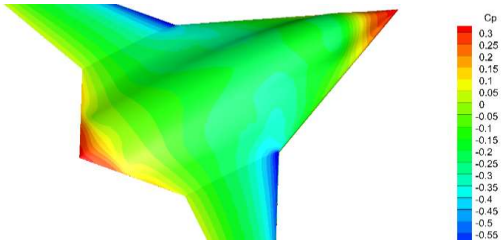

Figure 1. Cloud chart of CFD numerical simulation.

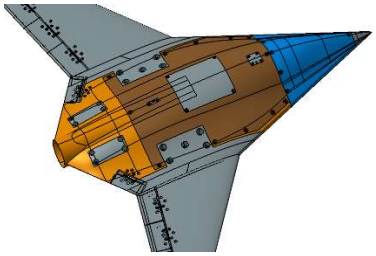

Figure 2. Wind tunnel experiment model.

2.2. Comparison of Longitudinal Aerodynamic Data

The comparison of longitudinal aerodynamic curves between numerical simulation and wind tunnel experiment is shown in Figure 3~Figure 5. It can be seen that:

a) The slope of lift coefficient curve has certain deviation;

b) The drag coefficient curve is basically consistent;

c) The slope deviation of the pitching moment coefficient curve is large, that is, there is a certain gap in the aerodynamic focus point.

The comparison of longitudinal aerodynamic data such as lift line slope $C_{L\alpha}$, zero drag coefficient C_{D0}, aerodynamic focus point C_{mCL} and zero-lift pitching moment coefficient C_{m0} are shown in Table 1, and it can be seen that the C_{D0} deviation is within 3.0%, while the maximum deviation of $C_{L\alpha}$, C_{mCL} and C_{m0} is 7.3%, -2.37% c_A and 0.0031.

2.3. Data Difference Analysis

The reasons for the deviation of longitudinal data are analyzed below to lay a technical foundation for the relevant correction of wind tunnel experiment and numerical simulation data.

2.3.1. Causes of $C_{L\alpha}$ Deviation.

The main reason for the deviation of lift coefficient between wind tunnel experiment and numerical simulation is the difference of model state, as shown in Figure 6. The experiment model is the shape state of the cutting rudder surface, and the simulation model is the complete shape state. Due to the difference of the model shape, there is a difference in the aerodynamic integration surface, and at the same time, the flow state of the air flow at the trailing edge of the wing-body is deviated, which causes the difference in the pressure distribution of the trailing edge of the wing body, and the slope of the lift line is different.

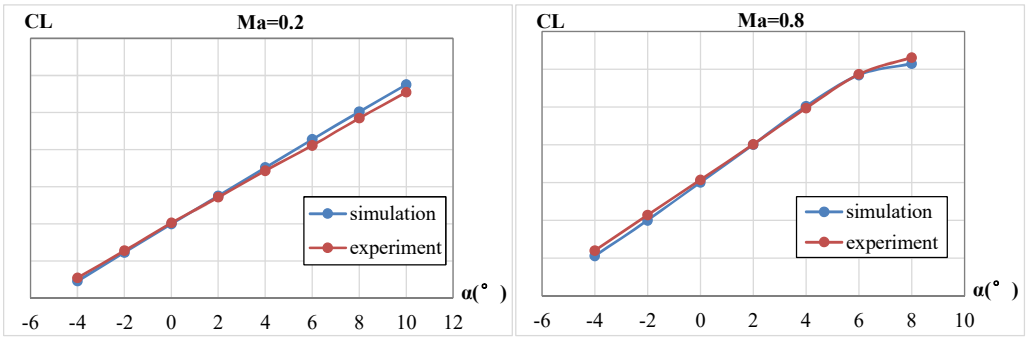

Figure 3. Comparison of lift coefficient curve between simulation and experiment.

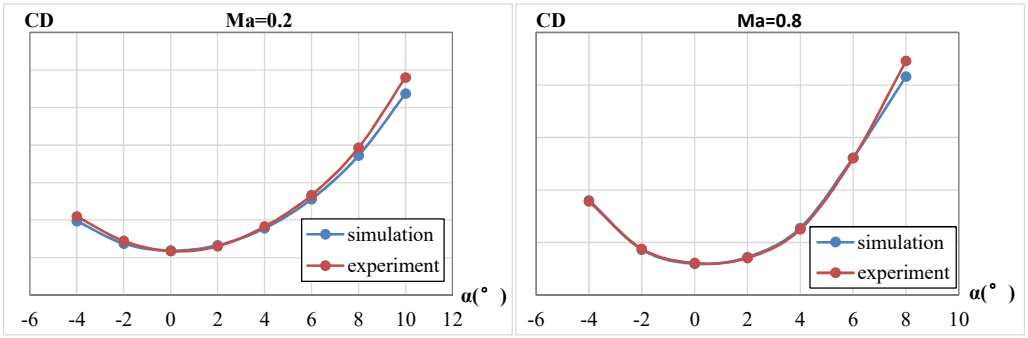

Figure 4. Comparison of drag coefficient curve between simulation and experiment.

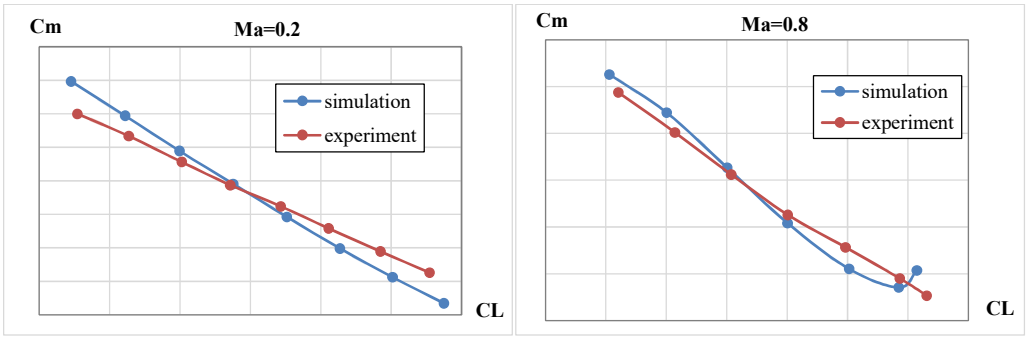

Figure 5. Comparison of pitching moment coefficient curve between simulation and experiment.

Table 1. Difference of longitudinal derivatives between simulation and experiment.

Ma	$\triangle C_{L\alpha}$	$\triangle\alpha_0(°)$	$\triangle C_{D0}$	$\triangle C_{mCL}$	$\triangle C_{m0}$	△Re
0.2	6.35%	0.037	1.24%	-1.55% c_A	0.0031	581%
0.4	3.90%	0.147	-0.63%	-1.77% c_A	-0.0010	575%
0.6	5.25%	0.124	-2.20%	-1.89% c_A	-0.0008	338%
0.8	7.30%	0.153	-1.88%	-2.37% c_A	0.0013	338%

Figure 6. Comparison between simulation model and experiment model.

2.3.2. Causes of C_{mCL} Deviation.

By analyzing the deviation of wind tunnel experiment and numerical simulation state, it can be concluded that there are two main reasons for the deviation:

a) Model state difference: due to the difference of model shape, there are differences in aerodynamic integral surface and trailing edge pressure distribution. At the same time, the force arm of the trailing edge of the wing and the fuselage is longer, which has obvious influence on the acting point of lift increment, namely the aerodynamic focus;

b) Reynolds number difference: the scaled model is used in the wind tunnel experiment and the atmospheric pressure is 0 altitude environment, while the full-size model is used in the numerical simulation and the atmospheric pressure is the real high-altitude environment, which makes the wind tunnel experiment Reynolds number 1~2 orders of magnitude lower than the numerical simulation Reynolds number. Due to the difference of Reynolds number, the flow characteristics of the fuselage and the wing have changed, which affects the aerodynamic focus point.

2.3.3. Causes of C_{m0} Deviation.

The main reason for the C_{m0} deviation between the wind tunnel experiment and the numerical simulation is the difference in the afterbody state, as shown in Figure 7. The wind tunnel experiment model adopts tail support mode, which destroys the afterbody; and the afterbody of numerical simulation is in the state of smooth and blocked cone. Due to the difference of the afterbody, the flow state of the air flow in the rear body is deviated, resulting in the difference of the pressure distribution. Because of the long force arm of the afterbody, the impact on the zero lift moment is more obvious.

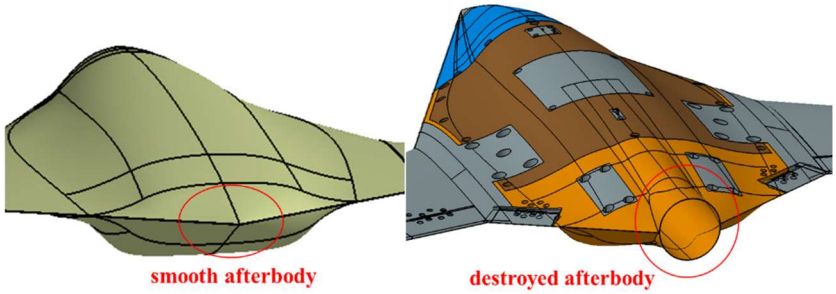

Figure 7. Comparison of afterbody differences between simulation and experiment.

3. Aerodynamic Data Correction

According to the analysis results in Section 2, the large deviation between wind tunnel experiment and numerical simulation of flying wing aircraft with small aspect ratio is the lift coefficient and pitching moment coefficient. Therefore, the lift coefficient and pitching moment coefficient are mainly corrected.

3.1. The Correction Method

3.1.1. The Correction Method of Lift Coefficient.

According to the curve of lift coefficient C_L changing with the angle of attack α, the C_L changes linearly with the C_L. The expression of C_L is:

$$C_L = C_{L\alpha} * \alpha + C_{L\alpha=0^\circ} \tag{1}$$

Since the lift coefficient at zero angle of attack is not corrected, the corrected lift coefficient can be expressed as

$$C_{L\ \text{correct}} = (C_{L\alpha} + \Delta C_{L\alpha}) * \alpha + C_{L\alpha=0^\circ} = C_L + \Delta C_{L\alpha} * \alpha \tag{2}$$

Therefore, the correction of lift coefficient is mainly to correct the lift line slope. The core of correction is to obtain the lift line slope deviation caused by all influencing factors, namely $\triangle C_{L\alpha}$.

3.1.2. The Correction Method of Pitching Moment Coefficient.

According to the curve of pitching moment coefficient C_m changing with lift coefficient C_L, the pitching moment coefficient changing with lift coefficient is basically linear, so the pitching moment coefficient C_m can be expressed as:

$$C_m = C_{mCL} * C_L + C_{m0} \tag{3}$$

Before correcting the pitching moment coefficient, it is necessary to fit and interpolate the corresponding C_m^* of $C_{L\ \text{correct}}$ according to the relationship between Cm and CL, so C_m^* can be expressed as:

$$C_m^* = C_{mCL} * C_{LCorrection} + C_{m0} \tag{4}$$

Therefore, the corrected pitching moment coefficient can be expressed as:

$$\begin{aligned} C_{mCorrection} = C_{mCLCorrection} * C_{LCorrection} + C_{m0Correctio} &= (C_{mCL} + \Delta C_{mCL}) * C_{LCorrection} + \\ (C_{m0} + \Delta C_{m0}) &= C_m^* + \Delta C_{mCL} * C_{LCorrection} + \Delta C_{m0} \end{aligned} \tag{5}$$

Therefore, the correction of pitching moment coefficient is mainly to correct the aerodynamic focus and zero-lift moment coefficient. The core of the correction is to obtain the deviation of the aerodynamic focus and zero-lift moment coefficient caused by all influencing factors, namely $\triangle C_{mCL}$ and $\triangle C_{m0}$.

3.2. Correction Values Acquisition

3.2.1. $\triangle C_{L\alpha}$ Acquisition.

The difference of lift coefficient is mainly derived from the influence of model state deviation. The lift line slopes $C_{L\alpha\ \text{model1}}$ and $C_{L\alpha\ \text{model2}}$ of the experiment model (trimmed surface) and the numerical simulation shape (complete surface) are obtained by numerical simulation, so the lift line slope deviation affected by the model state deviation is $\triangle CL\alpha = C_{L\alpha\ \text{model1}} - C_{L\alpha\ \text{model2}}$.

3.2.2. $\triangle C_{mCL}$ Acquisition.

The aerodynamic focus $C_{mCL\ model1}$ and $C_{mCL\ model2}$ of the experiment model state (trimmed surface) and the numerical simulation shape state (complete surface) are obtained by numerical simulation, so the aerodynamic focus deviation affected by the model state deviation is $\triangle C_{mCL\ 1}= C_{mCL\ model1}- C_{mCL\ model2}$.

The aerodynamic focus at different Reynolds numbers is obtained by numerical simulation, and the relationship between the aerodynamic focus and Reynolds number is obtained.

When Re≤4.6×106, the formula of C_{mCL} is:

$$C_{mCL} = -0.0061 * \left(\lg\left(\mathrm{Re}\right)\right)^{1.1955} \tag{6}$$

When Re≥4.6×106, the formula of C_{mCL} is:

$$C_{mCL} = -0.0007 * \left(\lg\left(\mathrm{Re}\right)\right)^{2.3082} \tag{7}$$

The aerodynamic focus $C_{mCL\ Re1}$ and $C_{mCL\ Re2}$ at the experiment Reynolds number and the simulation Reynolds number are calculated according to the above formula, so the aerodynamic focus deviation affected by Reynolds number is $\triangle C_{mCL\ 2}= C_{mCL\ Re1}- C_{mCL\ Re2}$. The focus correction can be obtained by summing the aerodynamic focus deviation caused by all influence: $\triangle C_{mCL}=\triangle C_{mCL\ 1}+\triangle C_{mCL\ 2}$.

3.2.3. $\triangle C_{m0}$ Acquisition.

The deviation of the zero-lift pitching moment coefficient mainly comes from the difference of the afterbody state of the model, the zero-lift pitching moment coefficient $C_{m0\ model1}$ and $C_{m0\ model2}$ of the experiment state and the numerical simulation state are obtained through numerical simulation, so the deviation of the zero-lift pitching moment coefficient affected by the afterbody state is $\triangle C_{m0}= C_{m0\ model1}- C_{m0\ model2}$.

All correction values are shown in Table 2.

Table 2. Correction values at different Mach numbers.

Ma	$\triangle C_{L\alpha}$	$\triangle C_{mCL}$	$\triangle C_{m0}$
0.2	-0.0041	0.0165	-0.0028
0.4	-0.0033	0.0176	0.0012
0.6	-0.0047	0.0183	0.0007
0.8	-0.0061	0.0214	-0.0010

3.3. Corrected Results and Comparative Analysis

Comparison of aerodynamic curves between corrected numerical simulation and wind tunnel experiment is shown in Figure 8~Figure 9, the comparison of of longitudinal aerodynamic data is shown in Table 3. It can be seen that the lift coefficient curve and pitching moment coefficient curve of the corrected numerical simulation are in good agreement with the wind tunnel experiment. The deviation of the lift line slope $C_{L\alpha}$ is within 1%, the deviation of the aerodynamic focus C_{mCL} is within 0.5% c_A, and the deviation of the zero-lift pitching moment coefficient C_{m0} is within 0.0004, which meets the requirements of engineering accuracy.

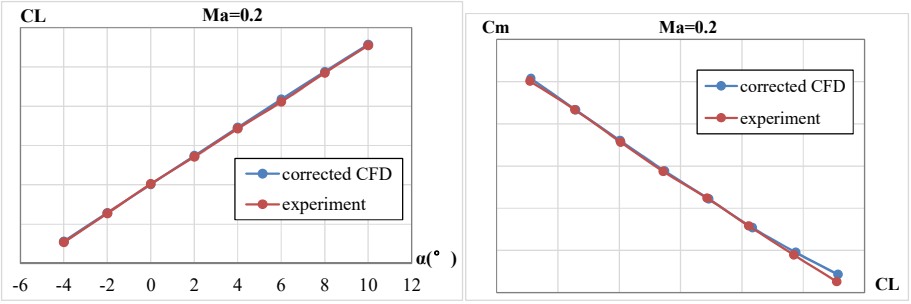

Figure 8. Comparison of C_L~α curve between corrected simulation and experiment.

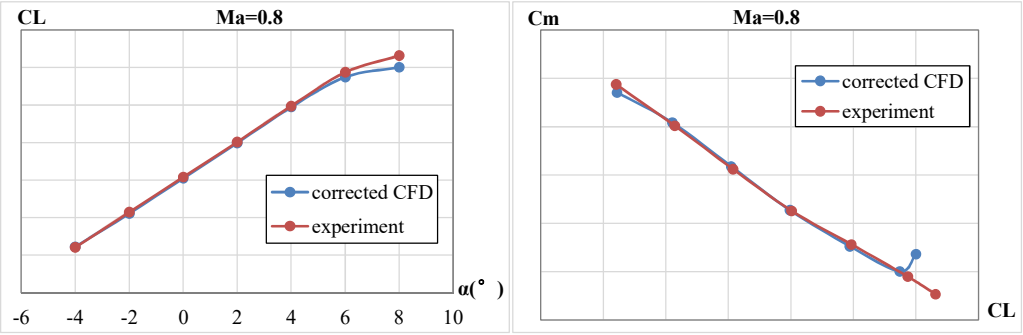

Figure 9. Comparison of C_m~ C_L curve between corrected simulation and experiment.

Table 3. Difference of longitudinal derivatives between corrected simulation and experiment.

Ma	$\triangle C_{L\alpha}$	$\triangle C_{mCL}$	$\triangle C_{m0}$
0.2	0.69%	0.10% c_A	0.0002
0.4	-0.39%	-0.01% c_A	0.0002
0.6	-0.49%	-0.06% c_A	-0.0001
0.8	0.75%	-0.23% c_A	0.0004

4. Conclusion

By comparing and analyzing CFD numerical simulation data and wind tunnel experiment data of small aspect ratio flying wing layout, the difference of longitudinal aerodynamic characteristics between simulation and experiment is obtained. After correction of simulation data, it is in good agreement with wind tunnel experiment data, which verifies the rationality and accuracy of comparative correction method. For the small aspect ratio flying wing configuration, the combination of numerical simulation and comparative correction can replace the wind tunnel experiment to obtain longitudinal aerodynamic data. The difference law and correction method of lateral heading and rudder surface efficiency characteristics between simulation and experiment, as well as the correction system of aerodynamic data applied to real aircraft flight conditions, are the direction of further research.

References

[1] Y. Yu, Y Huang and Z. Zhou, Aerodynamic design of a flying-wing aircraft, ACTA Aerodynamic Sinica, 2017, 35(6): 832-836.

[2] H. Wang and J. Bai, Design Essentials Research of the Flying-wing Configuration, Science Technology and Engineering, 2009, 9(12): 3570-3573.

[3] K. Yue, Y. Zhang and L. Cheng, Numerical Simulation of Aerodynamic Characteristics for Double-all-wing Unmanned Aerial Vehicle Based on Computational Fluid Dynamics, Journal of System Simulation, 2021, 33(7): 1654-1660.

[4] Y. Li, H. Liu, and Y. Huang. Investigation on the correlation of high-speed force test results of flying-wing calibration model with low-aspect ratio, ACTA Aerodynamic Sinica, 2016, 34(1): 107–112.

[5] J. Su, Y. Huang and S. Zhong, Research on flow characteristics of low-aspect-ratio flying-wing at transonic speed, ACTA Aerodynamic Sinica, 2015, 33(3): 307-312.

[6] Z. Ma, Z. Wang and X. Zhao, Application of airfoil test and numerical simulation in transonic wind tunnel, Experimental Technology and Management, 2020, 37(5): 128-131.

[7] Y. Liu, X Zhao and Z. Jiang, The computational and experimental investigation on winglets of a low speed aircraft, Journal of Experiments in Fluid Mechanics, 2015, 29(1): 55-59.

[8] X. Liu, Y. Lu and X. Zhang, Study on Aerodynamic Characteristics of Folding Wing Based on Wing Tunnel Experiment and CFD Method, Air&Space Defense, 2021, 4(1): 77-82.